WELDING RESEARCH

SUPPLEMENT TO THE WELDING JOURNAL, SEPTEMBER 1977

Sponsored by the American Welding Society and the Welding Research Council

Effect of Inadequate Joint Penetration on Fatigue Resistance of High-Strength Structural Steel Welds

Inadequate joint penetration defects as small as 0.5 mm (0.02 in.) wide reduce fatigue life below the normal expectancy for sound welds

BY Y. TOBE AND F. V. LAWRENCE, JR.

ABSTRACT. Zero-to-tension fatigue tests were carried out on double-V butt welds of ASTM A514 steel plate, 20 mm (0.79 in.) in thickness, which contained full-length lack of penetration (LOP) defects. The fatigue crack initiation and propagation portions of life were experimentally separated. Compression-to-tension fatigue tests were carried out on plane plate, as-welded sound joints and reinforcement-removed welds to experimentally determine the fatigue strength reduction factor (K_f) of the LOP defects.

LOP defects as small as 0.5 mm wide had a profound effect on fatigue life. The fatigue crack initiation life was found to be short—only 10% of the total life—and could be predicted using fatigue crack initiation concepts. The use of $K_{f_{max}}$, the maximum possible fatigue strength reduction factor, was found to be appropriate.

Introduction

Background

The fatigue resistance of welds is usually inferior to that of the metals which they join for at least two reasons:

1. The external discontinuities associated with the weld reinforcement or weld bead provide a very severe fatigue notch in butt, fillet, and lap welds; the fatigue resistance of the joint is controlled by the geometry of this notch—and unless the notch can be removed or modified by grinding or gas-tungsten-arc (GTA) dressing, for example, the fatigue life of the weldment is essentially fixed for a given loading condition.

2. Internal defects such as inadequate joint penetration (described here as lack of penetration (LOP)), lack of fusion (LOF), weld cracks, and others can provide the critical fatigue notch which determines the fatigue life of the weld; planar defects such as LOP, LOF, and cracks are particularly serious in this regard.

Because of the severity of the fatigue notch provided by external discontinuities, internal defects are not always the most serious and generally do not become critical until they become very large or until the weld reinforcement is removed, allowing the internal defect to control fatigue life.

Y. TOBE is Research Scientist, First Research Center, Japan Defense Agency, Tokyo, Japan, and F. V. LAWRENCE, JR., is Associate Professor of Civil Engineering and Metallurgy, University of Illinois at Urbana-Champaign, Urbana, Illinois

Purpose

The purposes of the study described in this paper were:

1. To determine the influence of LOP defects on the fatigue life of high-strength steel butt welds.
2. To determine experimentally the fractions of fatigue life devoted to crack initiation and crack propagation.
3. To analytically predict the initiation and propagation portions of life.
4. To determine the influence of clustered porosity on total fatigue life.

Approach

In this investigation, zero-to-tension ($R = 0$, R being the ratio of the minimum to maximum stress level) fatigue tests were carried out on double-V butt welds of ASTM A514

Table 1—Chemical Compositions of Base Metal (A514-F Plate) and Filler Metal (1.6 mm Bare Electrode)[a], Wt-%

	Base metal[b]	Filler metal
C	0.16	0.08
Si	0.23	0.46
Mn	0.82	1.70
P	0.012	0.005
S	0.019	0.009
Cu	0.27	—
Ni	0.76	2.40
Cr	0.54	0.05
Mo	0.47	0.50
V	0.06	0.02
B	0.004	—
Ti	—	0.025
Al	—	0.003

[a]Compositions supplied by manufacturer.
[b]Ladle composition.

Table 2—Small Specimen Tensile Properties for Base Metal and Weld Metal

		Yield strength S_y, MPa	Ultimate strength S_u, MPa
Base metal:[a]	Longitudinal	762.9	842.3
	Transverse	730.5	846.2
Weld metal[b]		871.7	966.9

[a]Overall specimen length—102 mm (4.02 in.); gage length—25.4 mm (1 in.); reduced section diameter—5.66 mm (0.22 in.)
[b]Overall specimen length—127 mm (5 in.); gage length—25.4 mm (1 in.); reduced section diameter—7.98 mm (0.314 in.); heat input—1.2 kJ/mm.

steel plate, 20 mm (0.79 in.) in thickness, which contained various width, full-length LOP defects. The initiation and propagation portions of the fatigue life were experimentally separated.

Compression-to-tension (R = −1) fatigue tests were carried out on plain plate, as-welded sound joints, and reinforcement-removed welds with several sizes of LOP defects to experimentally determine the fatigue strength reduction factor (K_f) of the toe of the weld and LOP defects.

Experimental Procedures

Materials and Test Specimen Fabrication

Test specimens were made from 20 mm (0.79 in.) thick ASTM A514 steel plates with the chemistry and nominal mechanical properties given in Tables 1 and 2. Table 1 also gives the chemistry of the 1.6 mm (1/16 in.) diameter Murex Hyloy 110 bare electrode which was used. The mechanical properties of deposited weld metal depend upon heat input, and the mechanical properties typical for a 1.2 kJ/mm heat input are given in Table 2.

Test specimen blanks were oxygen cut from plate stock keeping the rolling direction parallel to the eventual tensile axis. The blanks were sawed in half, and the edges were prepared with a 60 deg double-V edge preparation having oversize root faces (lands). The halves were welded using one pass per side, 98 C (208 F) preheat and interpass temperatures, Ar + 2%O_2 shielding gas, a 1.2 kJ/mm heat input, and zero root gap.

For land sizes larger than 2 mm (0.08 in.), the welding did not completely penetrate the root, resulting in the creation of full-length, LOP defects ranging from 1 to 8 mm (0.04 to 0.31 in.) in width ($2a_o$) which was oriented perpendicular to the tensile axis—Fig. 1. The welded test specimens were machined to the dimensions shown in Fig. 2.

Figure 3 shows a typical weld profile. The test specimens were fatigue-tested with the reinforcement intact, except for a few compression-to-tension (R = −1) tests for which it was removed by surface grinding. The test specimens were X-ray radiographed prior to testing to ensure the presence of the intended LOP and the absence of other, unintended defects.

In addition to the specimens containing full-length LOP defects described above, sound weld (containing no LOP) and plain plate test pieces of similar dimensions were prepared. The following code was used to identify the various types of test pieces:

P—plain plate with mill scale intact

W—sound welds with weld reinforcement intact

LN—test pieces with weld reinforcement intact and full-length LOP defects

LF—reinforcement-removed test pieces containing full-length LOP defects.

Fatigue Testing

All fatigue tests were performed under load control using a closed-loop, hydraulic test system. Specimens were mounted in the test frame and gripped with self-aligning grips. Testing was carried out under ambient laboratory conditions at a rate of 1 to 15 Hz. The load cycle was zero-to-tension (R = 0) for the W and LN test pieces and compression-to-tension (R = −1) for the long-life W and LF tests.

Strains near the LOP of some LN test pieces were monitored by strain gages (Micro Measurements EA-06-031CF-120) mounted 2 mm (0.08 in.) from the tip of the LOP defect—Fig. 3. The peak dynamic strains were monitored during the test and changes in these readings indicated a small enlargement of the original LOP defects. The significance of these strain changes in terms of crack advance was determined by heat-tinting and ink-stain methods. The initial size of the LOP defect was measured on the fracture surface.

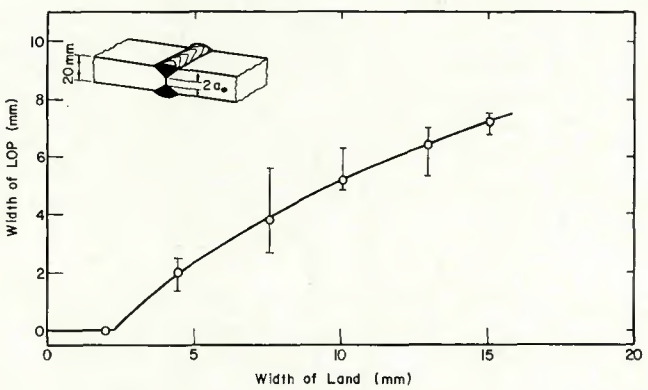

Fig. 1—Relationship between the width of edge preparation land and the width of the LOP defect obtained after welding

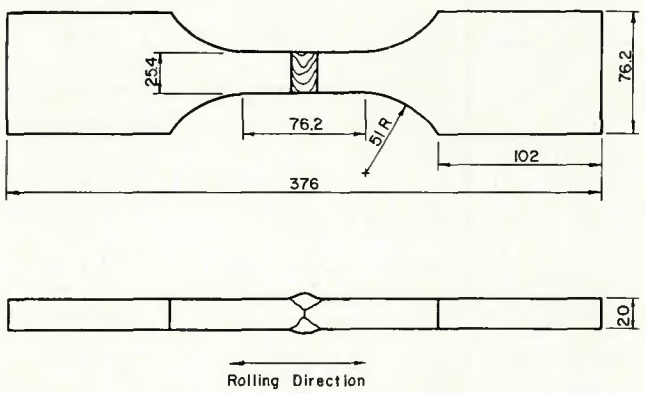

Fig. 2—Machined dimensions of test specimens. All dimensions in millimeters

Results

Fatigue Data

Tables 3, 4, and 5 give the results of all the fatigue tests. Table 3 gives the results for sound welds (R = 0) (W series). Table 4 gives the results of (R = 0) tests on welds with reinforcement intact containing full-length LOP defects (LN series), and Table 5 gives results for long-life (R = −1) tests run to experimentally determine the fatigue strength reduction factor (K_f).

The S-N diagram in Fig. 4 compares the results of the sound weld (W series) tests with data from the literature.[1] The test results lie within the 99% confidence limits for A514 butt welds and are thus typical for such welds.

Figure 5 shows the test data for the welds containing LOP defects (LN series); the data confirm the serious effect that such defects may have on fatigue resistance. The size of the LOP influenced life greatly, with the effect ranging from a slight reduction in life to as much as an order of magnitude reduction.

Figure 6 shows the results of compression-to-tension fatigue tests (R = −1) on plain plate, sound welds, and welds containing LOP defects.

Fatigue Crack Initiation and Propagation Locations

Figures 7 and 8 are macrographs of the fatigue crack initiation and propagation locations in the sound (W series) and LOP containing (LN series) test pieces. Figure 7 shows several toe initiation sites typical of the sound welds and welds containing very small LOP defects. It is interesting to note that initiation and early crack growth often occurred in the weld metal.

Figure 8 shows the influence of LOP

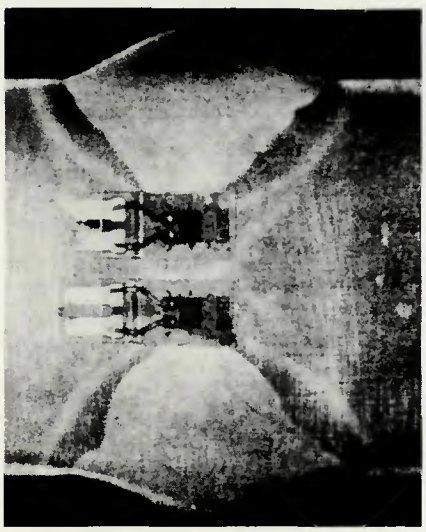

Fig. 3—Profile of LOP containing weld. LOP is not visible. Strain gages are mounted approximately 2 mm from tips of LOP

Table 3—Results of (R = 0) Fatigue Tests on Sound Welds With Reinforcement Intact

Specimen	Stress, MPa	Total fatigue life, cycles	Fracture mode: Crack initiation site	Fracture mode: Crack propagation path
W-5	412	215,000	toe (in WM)	WM → HAZ
W-7	412	159,000	toe (in WM)	Bond → HAZ
W-8	206	4,930,000	none	none
W-9	412	110,000	toe	HAZ
W-10	275	1,050,000	none	none
W-10[a]	309	1,030,000	toe	HAZ
W-12	240	4,950,000	none	none
W-12[a]	275	730,000	toe	HAZ
W-13	275	319,000	toe (in WM)	WM → HAZ

[a]Retested at higher stress level

Table 4—Results of (R = 0) Fatigue Tests on As-Welded Test Pieces Containing Full Length LOP Defects

Specimen	Width at LOP, $2a_o$, mm	Gross stress range, MPa	Total fatigue life, cycles	Fracture mode: Crack initiation site	Fracture mode: Crack propagation path
LN-14	2.01	412	13,100	LOP	WM
LN-15	1.78	206	252,000	LOP	WM
LN-16	1.21	206	256,000	LOP (+ toe)	WM (LOP)
LN-17	1.68	206	184,000	LOP	WM
LN-18	1.88	206	166,000	LOP	WM
LN-19	0.89	412	28,200	LOP (+ toe)	HAZ (toe) WM (LOP)
LN-20	0.50[a]	412	57,300	LOP (+ toe)[b]	HAZ
LN-22	7.00	206	70,600	LOP	WM
LN-23	6.40	412	4,070	LOP	WM
LN-24	6.67	206	82,900	LOP (+ toe)	WM (LOP)
LN-25	5.31	206	58,400	LOP (+ toe)	WM (LOP)
LN-26	7.09	412	3,190	LOP	WM
LN-27	7.28	412	3,370	LOP	WM
LN-28	7.51	206	49,000	LOP	WM
LN-29	6.76	206	38,300	LOP (+ toe)	WM (LOP)
LN-31	4.06	412	5,960	LOP	WM
LN-34	5.03	206	64,100	LOP (+ toe)	WM (LOP)
LN-35	4.75	412	6,210	LOP	WM
LN-43	2.47	206	143,000	LOP	WM
LN-45	1.41	412	22,100	LOP (+ toe)	WM (LOP)

[a]Length of the LOP—6 mm (0.24 in.)
[b]Crack initiated from two different toes, separately.

Table 5—Results of (R = −1) Fatigue Tests on ASTM A514 Plain Plates, Sound Welds and LOP Specimens

Specimen	Stress range, (MPa)	Total fatigue life, (cycles)	Fracture mode: Crack initiation site[a]	Fracture mode: Crack propagation path
P-2	412	5,000,000[c]	no sign of crack	
P-2[b]	480	5,000,000[c]	no sign of crack	
P-3	824	185,000	reduced section	
P-4	618	379,000	reduced section	
W-40	412	613,000	toe	HAZ
W-41	549	190,000	toes	HAZ
W-42	686	265,000	toe	HAZ
W-43	490	935,000	toe	HAZ
LF-30	127	889,000	LOP (2.68)	WM
LF-32	275	121,000	LOP (5.62)	WM
LF-33	176	547,000	LOP (2.95)	WM

[a]Numbers in parentheses indicate the average width of the full length LOP defects.
[b]Retested at higher stress level.
[c]Run out.

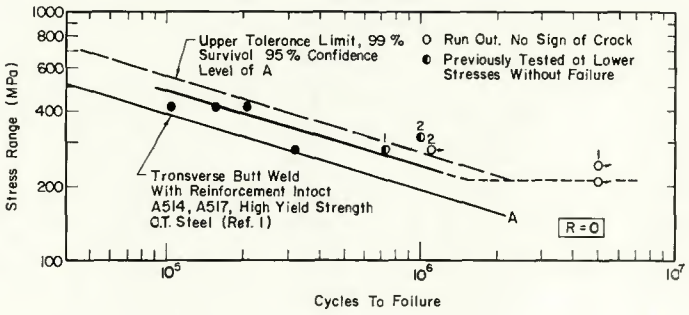

Fig. 4—S-N curve for sound welds (W series)

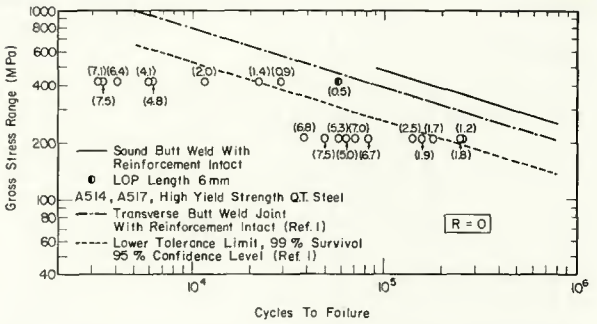

Fig. 5—Fatigue test results for butt welds containing full length LOP defects. The average LOP widths in millimeters ($2a_o$) are indicated in parentheses

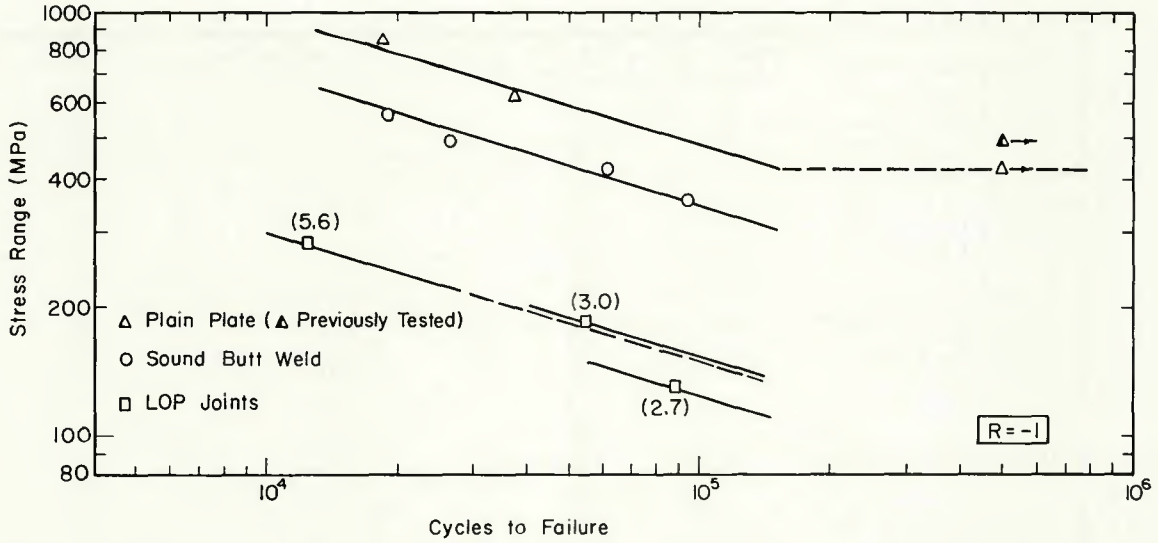

Fig. 6—Compression-to-tension fatigue data for plain plate, sound welds, and LOP containing welds. The LOP widths in millimeters ($2a_o$) are shown in parentheses

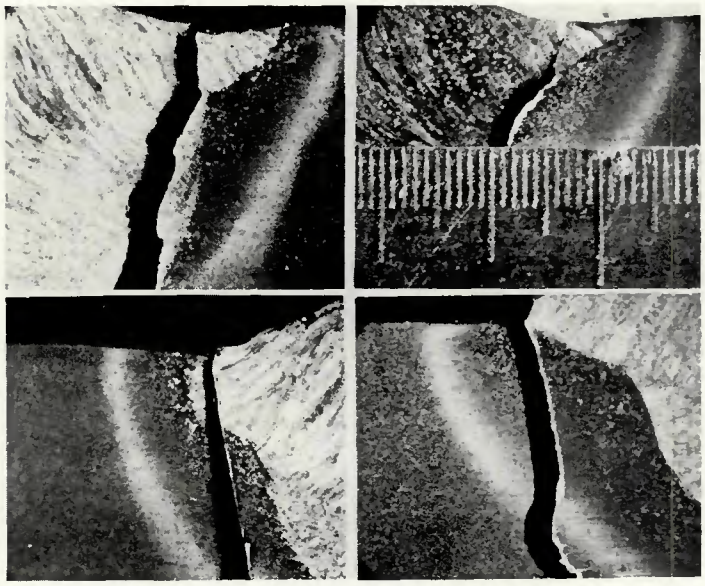

Fig. 7—Crack initiation sites and crack propagation paths for sound welds. (R = 0) (Gradations on scale in B are 0.01 in.). A (top left): W-5; N_T = 215,000; S = 412 MPa. B (top right): W-7; N_T = 159,000; S = 412 MPa. C (bottom left): W-13; N_T = 319,000; S = 275 MPa. D (bottom right): LN-19; N_T = 28,200; S = 412 MPa

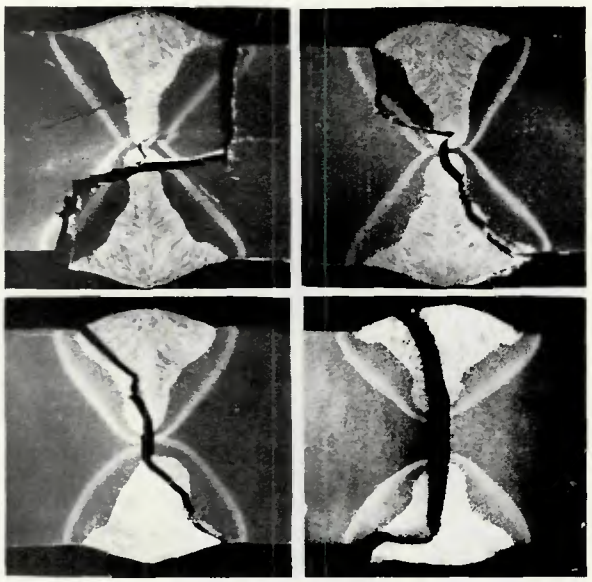

Fig. 8—Crack initiation sites and crack propagation paths for welds containing LOP defects. (R = 0) (magnification ≃ ×2.7). A (top left): LN-20 (0.5, 6); N_T = 57,300; S = 412 MPa. B (top right): LN-19 (0.9, full); N_T = 28,200; S = 412 MPa. C (bottom left): LN-14 (2.0, full); N_T = 13,100; S = 412 MPa. D (bottom right): LN-25 (5.3, full), N_T = 58,300; S = 206 MPa

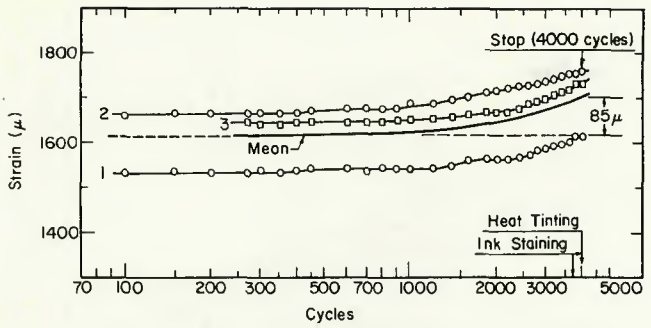

Fig. 9—Peak dynamic strain near the tips of LOP in Specimen LN-37 which was tested under a stress range of 206 MPa and contained a 6.3 mm width LOP. The strain change of 85 × 10^{-6} corresponded to a half width increase of 0.39 mm

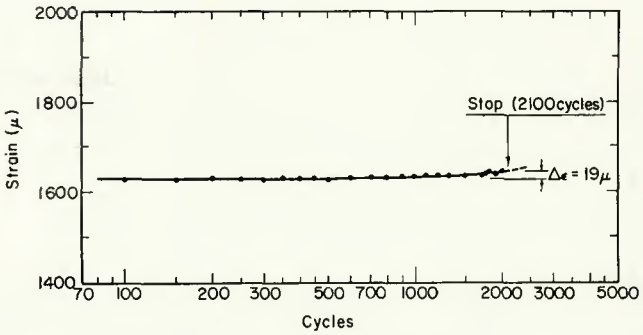

Fig. 10—Peak dynamic strain near tip of LOP in Specimen LN-36 which was tested under a stress range of 206 MPa and which contained a 4.8 mm width LOP. The strain change of 19 × 10^{-6} corresponded to a half width increase of 0.1 mm

Table 6—Measured Fatigue Crack Initiation and Fatigue Crack Propagation Lives

Specimen	Stress range R = 0, MPa	Defect width $2a_o$, mm	N_T, cycles	N_I (measured), cycles	N_P (measured), cycles
LN-17	206	1.68	184,000	12,500	171,500
LN-18	206	1.88	166,000	11,800	154,200
LN-22	206	7.00	70,600	1,850	68,750
LN-26	412	7.09	3,190	145	3,045
LN-27	412	7.28	3,370	135	3,235
LN-28	206	7.51	49,000	2,750	46,250
LN-29	206	6.76	38,300	2,050	36,750
LN-31	412	4.06	5,960	300	5,660
LN-34	206	5.03	64,100	3,750	60,350
LN-36	206	4.80	—	2,100	—
LN-37	206	6.30	—	1,600	—
LN-43	206	2.47	143,000	5,800	137,200
LN-45	412	1.41	22,100	2,450	19,650
LN-47	137	2.50	—	155,000	—

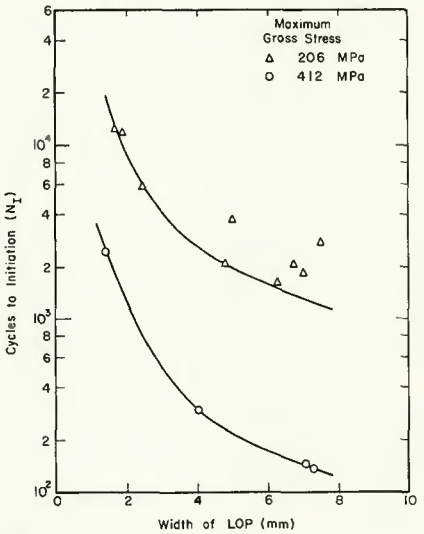

Fig. 11—Relationship between LOP width ($2a_o$) and measured fatigue crack initiation life (N_I)

size on the initiation sites and propagation paths for welds containing full-length LOP defects (LN series). At the largest LOP widths (Fig. 8D) the LOP clearly dominates; in all cases, however, there is some interaction between the toe and the LOP defect. At the smaller LOP widths (Figs. 8A and B), initiation and propagation at the weld toe dominate.

The initiation and propagation patterns are complex. However, it should be remembered that the final stages of fracture, during which these complex patterns develop, occur only during the very last stages of the fatigue life.

Detecting Crack Initiation and Early Growth

Figure 9 shows the typical peak strain histories of strain gages located approximately 2 mm (0.08 in.) from the tip of a LOP defect. The peak strain remains relatively constant during the early portions of the fatigue life but begins to increase after about 1000 cycles. At 4000 cycles, the specimen was removed from the test frame and cut in half lengthwise. One half was ink-stained and the other heat-tinted to determine the crack advance associated with the 85 × 10^{-6} peak strain increase. The specimen halves were then fractured in monotonic tension. Examination of the fracture surfaces revealed a 0.78 mm (0.03 in.) increase in LOP width. Heat-tinting and ink-staining methods gave the same result.

The increased strain reading is related either to the stresses associated

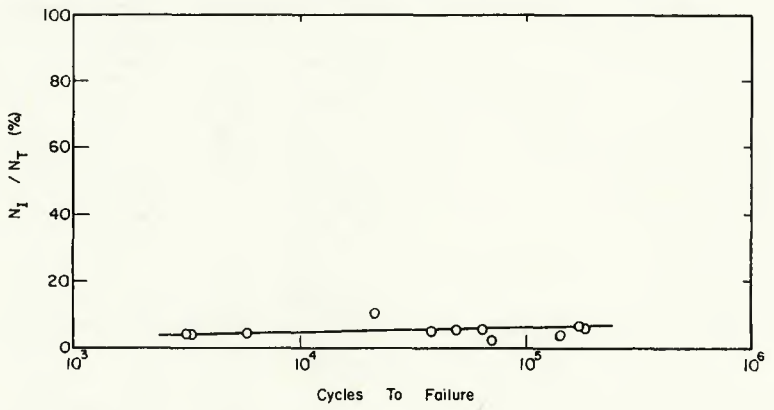

Fig. 12—Percentage of life devoted to fatigue crack initiation as a function of total life

Table 7—Low Cycle Fatigue Properties

E = 207,887 MPa
σ'_y = 600 MPa
σ'_f = 1359 MPa
e'_f = 0.595
b = −0.0785
c = −0.590
n' = 0.128
σ_f = 1406 MPa
$2N_{tr}$ = 6944 reversals

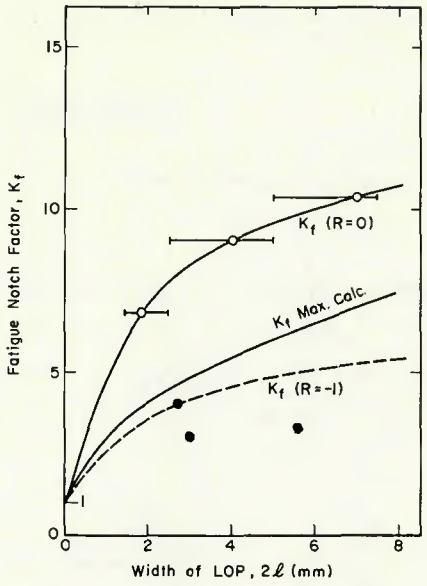

Fig. 13—Comparison of values of fatigue notch factor (K_f) derived from R = 0 and R = −1 long life fatigue tests with calculated values assuming $K_{f_{max}}$ conditions

with the tip of the advancing crack or to increases in the net section stress or both. A stress analysis of the state of stress in the vicinity of the strain gages revealed that, at the location 2 mm (0.08 in.) from the crack tip, the stress is approximately equal to the net section stress. Using the simplest approximation:

$$\Delta e \approx \frac{P}{EW}\left[\frac{1}{t-(2a_o+2\Delta a)}-\frac{1}{t-2a_o}\right] \quad (1)$$

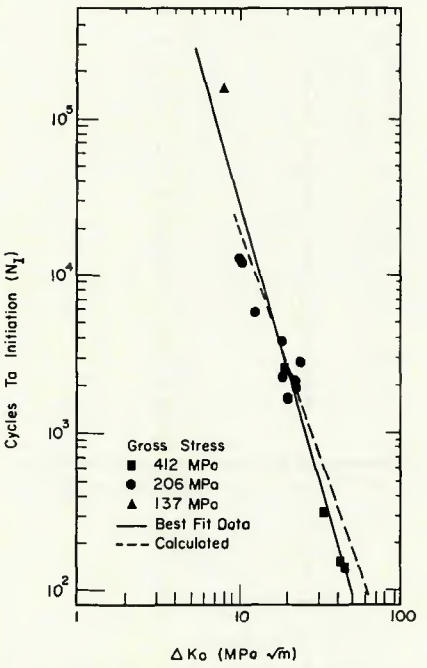

Fig. 15—Relationship between initial range in stress intensity factor ($\Delta K_o = S\sqrt{\pi a_o}$) and fatigue crack initiation life

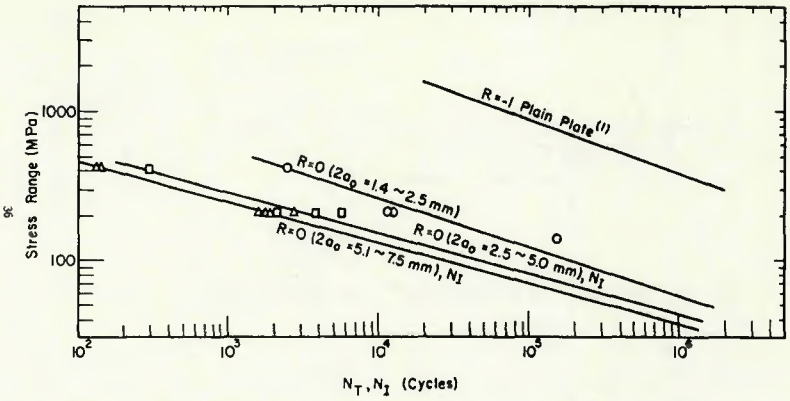

Fig. 14—Stress versus cycles to failure for plain plates (R = −1) and cycles to initiation for LN series containing LOP (R = 0)

where: Δe—strain increase due to a crack advance 2Δa; 2Δa—crack advance; $2a_o$—initial LOP width; t—weld thickness ≈ plate thickness; W—test piece width; E—Young's modulus; P—load on test piece.

This approximation predicts that if $2a_o$ equalled 4.8 mm (0.19 in.), for example, a crack advance (2Δa) of 0.254 mm would produce a strain change Δe of 22×10^{-6}. To test this prediction, specimen LN-36 was fatigued until the predicted strain change was observed—Fig. 10. The observed crack advance (2Δa) was 0.20 mm (0.008 in.) rather than the 0.254 mm (0.01 in.) predicted. In any case, a change of strain of 19×10^{-6} represents a very small (~0.1 mm) increase in LOP half width. This amount of crack growth which was adopted as an arbitrary division between crack initiation and early growth, and steady state fatigue crack propagation—was sensed in subsequent tests by the appropriate change in peak dynamic strain.

The measured crack initiation life (N_I), determined assuming a crack advance (Δa) of 0.127 mm as the division between initiation (and early crack growth) and fatigue crack propagation, is tabulated in Table 6 and plotted against LOP defect width in Fig. 11. The measured initiation life is relatively short and depends strongly on LOP defect width and the applied stress level.

The percentage of life devoted to initiation is plotted as a function of total life (N_T) in Fig. 12. The measured initiation life (N_I) is 10% or less of the total life.

Discussion

Fatigue Crack Initiation Life at LOP Defects

As seen in Table 7 and Fig. 12, the fatigue crack initiation life (N_I) is quite short. This result is not too surprising, since the LOP defects are flat, crack-like defects oriented in the worst possible attitude, i.e., perpendicular to the fluctuating tensile stress. Nonetheless, it is interesting to see whether this measurement and low cycle fatigue life predictions agree.

To estimate the fatigue crack initiation life (N_I) using low cycle fatigue concepts, several simplifying assumptions were made:

1. The mean stress was assumed to

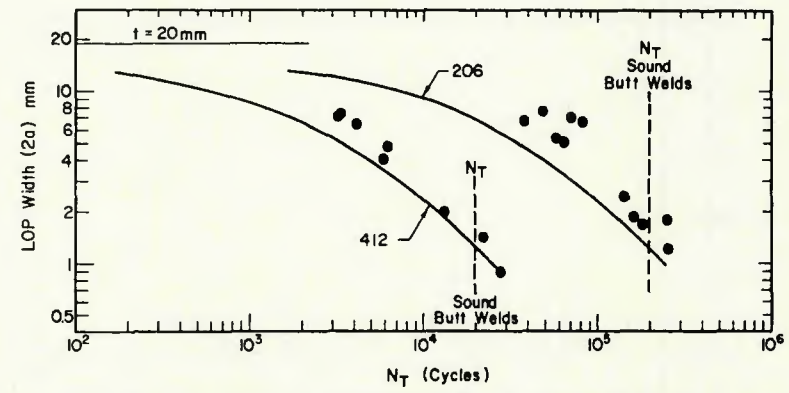

Fig. 16—Initial LOP width ($2a_o$) versus total life ($N_T \simeq N_p$). Solid curves were calculated using eq 14 ($C = 1.48 \times 10^{-10}$ ($MPa\sqrt{m}$), n = 3.32, K_c = 241 $MPa\sqrt{m}$). Vertical dashed lines indicate lower confidence limits for sound butt welds with reinforcement intact

decay to zero after very few cycles so that at the tip of the LOP, the mean stress is taken to be zero.

2. It was assumed that the elastic strains at the LOP tip are small relative to the plastic strains; this assumption should be valid if both the measured and calculated initiation lives are less than the transition fatigue life (N_{tr}) of the material, at which the elastic and plastic cyclic strains are equal by definition.

3. It was assumed that a modified Neuber relation estimates the product of stress and strain ($\sigma \cdot e$) at the tip of the LOP defect:[2,3]

$$\frac{(SK_f)^2}{E} = \sigma \cdot e \qquad (2)$$

where: S—remotely applied stress; K_f—fatigue notch factor; E—Young's modulus; σ—notch tip stress range; e—notch tip strain range.

The first difficulty is estimating K_f. Peterson's equation[4] gives a relationship between K_f and the elastic stress concentration factor (K_t) and requires knowledge of a microstructural parameter (A) and the notch root radius (r):

$$K_f = 1 + (K_t - 1)/(1 + (A/r)) \qquad (3)$$

and for an elliptical flaw:

$$K_t = 1 + 2(c/r)^{1/2} \qquad (4)$$

where: c = LOP half width; r = LOP tip radius.

Peterson's equation becomes:

$$K_f = 1 + 2(c/r)^{1/2}/(1 + (A/r)) \qquad (5)$$

Values of K_f predicted by this equation achieve a maximum value ($K_{f_{max}}$) for values of r equal to A.

$$K_{f_{max}} = 1 + (c/A)^{1/2} \qquad (6)$$

The maximum value of K_f is assumed to occur at some location at the tip of the LOP, constituting the most severe location or at least the most pessimistic assumption of the length of N_I. Values of "A" in Peterson's equation for steels are given in the literature and also by the relationship:[4]

$$A \text{ (in SI units)} \simeq 3.937 \times 10^{-5} (2068/S_u)^{1.8} \qquad (7)$$

Figure 13 compares K_f values calculated using $K_{f_{max}}$ (eq 6) and long-life fatigue test results. The K_f values calculated from R = −1 tests (Table 5 and Fig. 6) lie below the calculated $K_{f_{max}}$ values, but it must be remembered that the total life of these tests includes an unknown amount of propagation.

The LN series tests in which N_I was measured provide a second comparison. Using N_T for plain plate and N_I from the R = 0 tests (Fig. 14) gives a much higher calculated value of K_f, presumably because the N_T for the plain plate also include some propagation. Probably the best experimental values are provided by the R = −1 tests; as is seen in Fig. 13, the agreement between $K_{f_{max}}$ and these data is closest. Rewriting eq 2:

$$(S\,K_{f_{max}})^2 = 4\,E\,\sigma_a(\Delta e/2) \qquad (8)$$

where: σ_a = stress amplitude = $\Delta\sigma/2$; $\Delta e/2$ = total strain amplitude.

Now:

$$\Delta e/2 \approx \Delta e_p/2 = e'_f\,(2N_I)^c \qquad (9)$$

for lives less than N_{tr}. It is also true that:

$$\sigma_a = \sigma'_f\,(2N_I)^b \qquad (10)$$

where: $e_p/2$ = plastic strain amplitude; e'_f = fatigue ductility coefficient; c = fatigue ductility exponent; σ'_f = fatigue strength coefficient; b = fatigue strength exponent; N_I = crack initiation life.

Combining eqs 8, 9, and 10

$$(S\,K_f)^2 = 4\,E\,\sigma'_f\,e'_f[2N_I]^{b+c} \qquad (11)$$

or, using eq 6 for $K_{f_{max}}$ and recalling that $\Delta K_o \simeq S\sqrt{\pi a_o}$,

$$N_I \simeq \frac{1}{2}\left[\frac{\sqrt{4\pi A\,E\,\sigma'_f e'_f}}{\Delta K_o}\right]^{\frac{2}{|b|+|c|}} \qquad (12)$$

Values of N_I predicted by eq 12 and strain controlled fatigue data for one pass E110 weld metal (Table 7) are plotted as a dashed line in Fig. 15. As predicted by eq 12 the relationship between N_I and ΔK_o is a power law. The slope of the experimental data is −3, and the slope predicted by eq 12 (i.e., $2/|b| + |c|$) is −2.97. The agreement between experiment and calculation is better than would be expected.

Although the agreement may be fortuitous, several conclusions can be drawn: the mean stress must relax at the tip of the LOP defect, the strains at the tip of the LOP defect are predominantly plastic, and the use of $K_{f_{max}}$ is apparently appropriate.

Fatigue Crack Propagation Life

The major portion of life of the specimens containing LOP defects was devoted to fatigue crack propagation. The initiation life, while finite and predicted by low cycle fatigue concepts, was seen to be so short for the stresses and strains investigated that there is little difference between the total fatigue life (N_T) and the fatigue crack propagation portion of total life (N_p).

Table 6 lists the total, initiation, and propagation lives, and Fig. 16 plots the total fatigue life against LOP defect width ($2a_o$). The solid lines in Fig. 16 have been calculated using the power law relationship for fatigue crack growth:[5]

$$da/dN = C(\Delta K)^n \qquad (13)$$

and the stress intensity factor for a center-cracked plate having finite dimensions is defined by:

$$\Delta K = S\sqrt{\pi a}\,(\sec \pi a/2)^{1/2} \qquad (14)$$

This leads to an expression which predicts N_P as a function of stress range (S) and initial and final LOP defect half width (a_o, a_f):

$$N_P = \frac{1}{C}\int_{a_o}^{a_f} (S\sqrt{\pi a}(\sec \pi a/t)^{1/2})^{-n}\,da \qquad (15)$$

where t is the plate thickness, and the values of C and n (the materials properties in eqs 13 and 15) which best fit the experimental data were found to be:

$$n = 3.32;\ C = 4.68 \times 10^{-9} (\text{MPa}\sqrt{\text{m}})$$

These values are similar to those reported by Bucci et al.[6] for T-1 steel (base metal).

Influence of LOP on Fatigue Life

Cracklike defects such as LOP are serious defects which greatly reduce the fatigue life of welds in which they exist. As seen in Figs. 5, 11, 15, and 16, the influence of full-length LOP defects upon life is a very strong function of the width of the defect ($2a_o$). A major reason for the short lives produced by these defects is that the initiation portion of life is reduced to insignificant values due to the high stress concentration at the tip of the defect. Consequently, for specimens loaded above the threshold value of K (ΔK_{th}), the majority of life is spent in propagation.

Even the smallest defect studied—0.5 mm (0.02 in.) wide, 6 mm (0.24 in.) long (a less-than-full-length LOP, specimen LN-20)—resulted in a life shorter than the average for sound butt welds with reinforcement intact. If the fatigue resistance of sound butt welds is viewed from a statistical standpoint and the lower confidence limit for sound weld data is used as a criterion, then, as seen in Fig 5, LOP defects with widths ($2a_o$) slightly larger than 1 mm would be tolerable, because they would produce lives no shorter than the lower confidence limit for sound butt welds—Fig. 16.

Conclusion

Flat, cracklike defects such as LOP have a profound effect on the fatigue resistance of butt welds. Results of this study showed that LOP defects as small as 0.5 mm wide reduced the fatigue life below the normal expectancy for sound welds; however, LOP defects as large as 1 mm (0.04 in.) may be tolerated if the lower confidence limit for sound weld data is adopted as a criterion.

The initiation life of LOP defects, as defined and measured, was shown to be very short (less than 10% of total life) and could be predicted using fatigue crack initiation concepts and low-cycle fatigue data for E110 weld metal. The agreement between the measured and predicted initiation lives suggests that the mean stresses at the tip of the LOP defect decay rapidly and that the fatigue strength reduction factor (K_f) associated with the LOP is very close to the maximum possible K_t calculated using Peterson's equation.

The fatigue crack propagation portion of life was explained in terms of the power law for fatigue crack growth and was seen to occupy over 90% of the total life in the life range 10^3 to 10^6 cycles.

Acknowledgments

The authors gratefully acknowledge the support of the U. S. Army Construction Engineering Research Laboratory during the execution of this work. Mr. E. P. Cox, the contract monitor, provided useful guidance and criticism.

The authors thank the Japan Defense Agency for enabling Dr. Tobe to undertake this study during a year's visit at the University of Illinois.

References

1. Munse, W.H., et al, *Fatigue Data Bank and Data Analysis Investigation,* Structural Research No. 405 (University of Illinois at Urbana-Champaign, June 1973).

2. Mattos, R.J., *Estimation of the Fatigue Crack Initiation Life in Welds Using Low Cycle Fatigue Concept,* Ph.D. Thesis (University of Illinois at Urbana-Champaign, 1975).

3. Neuber, H., "Theory of Stress Concentration for Shear Strained Prismatical Bodies with Arbitrary Non-Linear Stress-Strain Laws," *Journal of Applied Mechanics,* (December 1961), p. 544.

4. Peterson, R.E., "Fatigue of Metals III—Engineering and Design Aspects," *Materials Research and Standards,* Vol. 6, No. 6 (February 1963), p. 313.

5. Paris, P.C., et al., "A Critical Analysis of Crack Propagation Laws," *Trans. ASME(D),* Vol 85, No. 4 (1963).

6. Bucci, R.J., et al., *Fatigue Crack Propagation Growth Rates Under a Wide Variation of ΔK for an ASTM A-517 Grade F (7-1) Steel,* ASTM STP 513 (American Society for Testing and Materials, September 1972).

WRC Bulletin 226

May 1977

A Review of Minor Element Effects on the Welding Arc and Weld Penetration

by S.S. Glickstein and W. Yeniscavich

Sporadic information has been reported on the effects of minor elements on the welding arc and weld penetration. A critical review of all the available literature pertaining to this subject matter has been undertaken in this report. Several studies have revealed that the addition of small amounts of halides to the base material significantly improves weld penetration. An attempt has also been made to provide some rationale for understanding how the properties of minor elements can affect the factors which influence weld penetration.

Publication of this paper was sponsored by the Welding Research Council.

The price of *WRC Bulletin 226* is $7.50 per copy. Orders should be sent with payment to the Welding Research Council, United Engineering Center, 345 East 47th St., New York, NY 10017.

WRC Bulletin 223

January 1977

Hot Wire Welding and Surfacing Techniques

by A. F. Manz

This WRC Bulletin is divided into two parts. The first part presents a non-mathematical description of the Hot Wire processes and their general characteristics. The second part presents a generalized in-depth mathematical treatment of electrode melt rate phenomena. In addition to describing Hot Wire electrode melting, Part II also presents considerable information concerning the general case of I-R heating of any moving electrode. Examples are given to demonstrate the utility of the derived equations in predicting the melt rates, temperature distribution and voltage drops of moving electrodes. Specific examples concerning Hot Wires are included.

Publication of this report was sponsored by the Interpretive Reports Committee of the Welding Research Council.

The price of *WRC Bulletin 223* is $7.50 per copy. Orders should be sent with payment to the Welding Research Council, United Engineering Center, 345 East 47th Street, New York, NY 10017.